Event coordinators:
Lauryna Šidlauskaitė Justas Kažys Jonas Kaminskas

PROCEEDINGS OF THE 20TH SIRWEC CONFERENCE, DRUSKININKAI, LITHUANIA (14-16TH JUNE 2022)

2022

EFFECTS OF SCREENING AND SKY VIEW FACTOR ON ROAD SURFACE TEMPERATURE FORECASTS

Virve Karsisto, Matti Horttanainen
Finnish Meteorological Institute, Erik Palménin aukio 1, 00560 Helsinki, *virve.karsisto@fmi.fi*, ORCID: 0000-0002-5212-1002

Summary

Road surroundings can affect significantly to the road surface temperature. In this study, the effects of including sky view factor and screening to the Finnish Meteorological Institute's (FMI) road weather model (RWM) are tested. According to the results, the effects vary greatly depending on the studied location. Even changing the lane can affect considerably to the road surface temperature. Shadowing increases the already negative bias in the forecasts in some cases, but at best it considerably decreases the RMSE during the day.

Introduction

Screening has a great effect on road surface temperature. During the daytime, the shadowed locations can be several degrees colder than locations exposed to the sun. On the other hand, obscured locations can remain warmer on clear nights due to the radiation emitted by the surroundings. Taking these effects into account in the road weather forecasts is an important step in making the forecasts more accurate. This can be done by determining sky view factor (SVF) and local horizon angles (LHAs) for the forecast location. The SVF means the fraction of the radiation reaching the surface from the radiation of the entire sky. The LHAs are determined as the angles between the flat surface and the visible horizon. There are two

common approaches to determine these values. The first uses fish-eye photographs that give 360° view of the location [1]. The second uses digital surface models (DSM), which are height maps in raster format [2]. The DSMs include buildings and vegetation in addition to terrain features. There have been some previous studies about how the SVF and/or LHAs affect to the road surface temperature forecasts [3,4]. However, there is still need for more excessive research in different environments.

The FMI's Road weather model (RWM) has thus fare expected open road surroundings, although some experiments with SVFs and LHAs have been made. In this study, the SVFs and LHAs were included to the FMI RWM and their effect to the road surface temperature forecasts was studied. The model was run for three winter periods (2018-2019, 2019-2020, 2020-2021) with and without SVFs and LHAs and the forecast verification results of the two runs were compared. The runs without SVFs and LHAs will be called as "Reference" and the runs including them as "Test". 23 road weather stations (RWS) with the SVFs varying between 0.72 and 0.98 were included in the study.

Data and Methods

DSMs generated from the National Land Survey of Finland's (NLS) laser scanning data [5] were used to determine the SVFs and LHAs at station locations. The laser data was processed to DSM using Lastools software [6]. Fig. 1 shows an example DSM for Salo Lakiamäki station in southern Finland. There are rock cuttings at both sided of the motorway, which makes it a rather shadowed location. Fig. 2 shows the LHAs calculated for the station with Grass software [7]. The LHAs were determined for both the southern and northern lanes and the forecasts were made for them

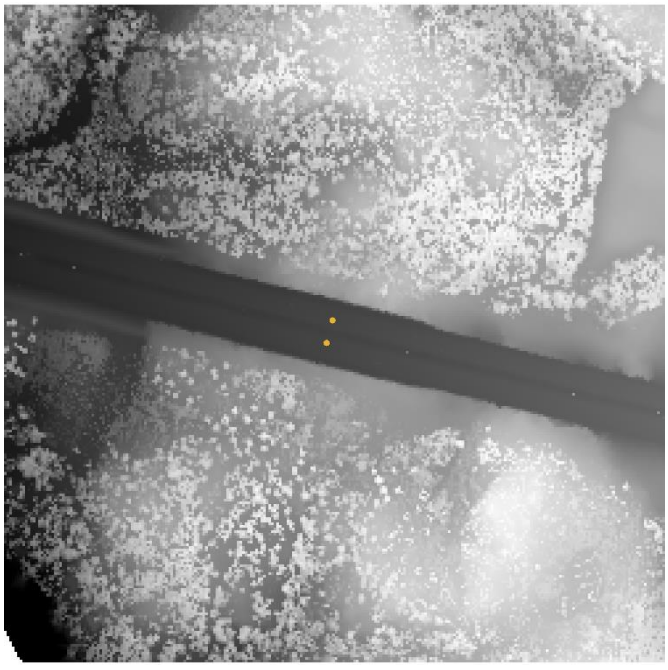

Fig. 1. The DSM determined from laser scanning data around Salo Lakiamäki RWS and the selected coordinate points for the simulations.

separately. On the southern lane the LHAs are clearly larger in the south than in the north, whereas the opposite is true for the northern lane. This causes large surface temperature differences during autumn and spring, when the northern lane is exposed to the sun but the southern lane is in shadow.

The FMI RWM is an one dimensional energy balance model which predicts surface temperature and road conditions [8]. As input, the model requires air temperature, wind speed, humidity, precipitation and incoming short and long wave radiation. Road surface temprature can be also used in the initialization. In this study, a shadowing algorithm and the SVF were added to the model. To calculate the modified radiation fluxes, direct short wave radiation and net long wave radiation were added to the input parameters. The shadowing algorithm reduces the direct solar radiation to zero when the sun elevation is lower than the LHA in the direction of the sun.

The SVF affects to the incoming diffuse short wave radiation, incoming long wave radiation and the long wave radiation emitted by the road surroundings following the equations used in the HIRLAM model [9].

The RWM runs consisted of a 48-h inititalization period where the input data was taken from the RWS observations and a 24-h forecast period where the input was taken from the MEPS (MetCoOp Ensemble Prediction System) forecast [10]. MEPS is a 3D numerical weather prediction model developed by the HIRLAM consortium. In case the the RWS had multiple surface temperature sensors, the model runs were run separately using each of their data in the initialization. The same sensor that was used in the initialization was also used in the verification. The exact coordinates of the RWS surface temperature sensors were unknown, so all the runs were done for two lanes separately. For example, if there were 2 sensors, a total number of 4

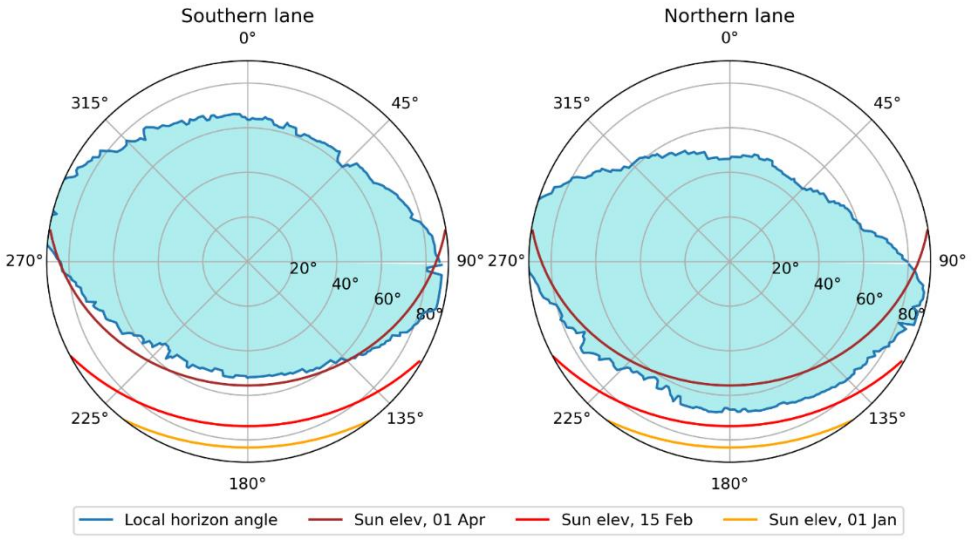

Fig. 2. The local horizon angels (blue line) at Salo Lakiamäki RWS on the southern (left figure) and the northern (right figure) lanes. The outer perimeter shows the direction so that the north is at 0°. The visible sky is shown in light blue color. Brown, red, and yellow lines show the sun elevation angels throughout days 1st April 2019, 15 February 2019, and 1st January 2019, respectively.

forecasts were made for one station. The simulations were done for three winter periods starting from October 2018 and ending to March 2021. Four forecasts with start times 03, 09, 15 and 21 UTC were done for each day.

Results

The daily behaviour of surface temperature forecast bias is clearly dependent on the lane and the sensor used in the initialization and verification (Fig. 3.). The reference simulations have warm bias during the day as they do not take screening into account. However, when the

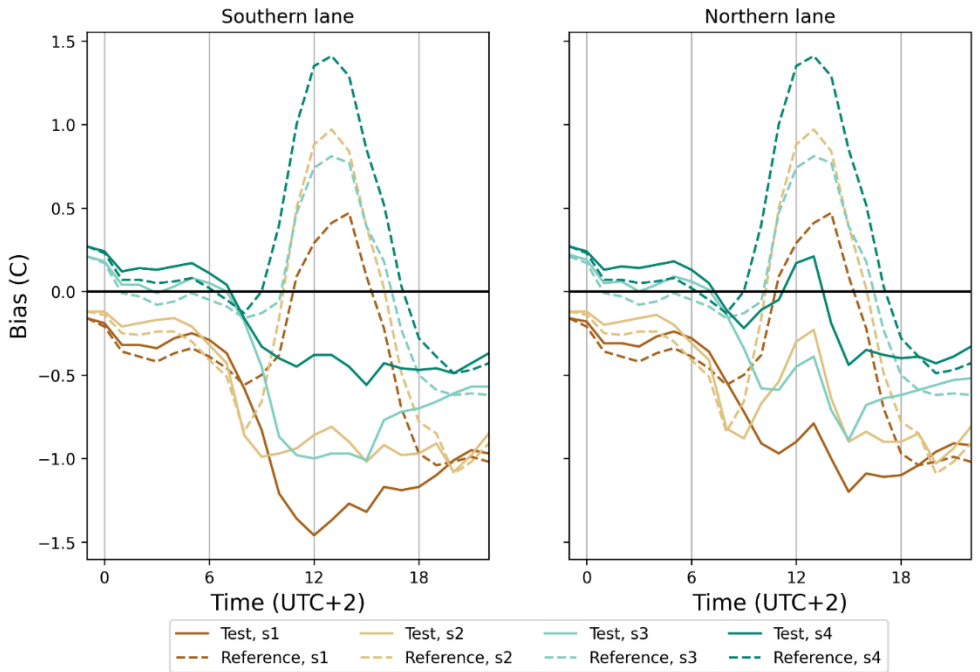

Fig. 3. Bias for Salo Lakiamäki station calculated for Octobers 2018-2020. The simulation start time was 21 UTC. The x-axis shows time of day in Finnish wintertime (UTC+2). Results for test runs are in continuous lines and for the reference runs in dashed lines. The left figure shows results for the southern lane and the right for the northern lane. Results for runs using sensor 1 are in brown, sensor 2 in light brown, sensor 3 in turquoise and sensor 4 in darker turquoise lines.

screening is taken into account the bias becomes negative for most sensors. The northern lane is warmer than the southern lane in the simulations as it is more exposed to the sun. It seems that the sensor 4 is in the most shadowed location as it has the least negative bias during the day for the test run and the most positive bias for the reference run. The sensor 1 seem to be in the most open location. During the night the radiation from the surrounding causes the test simulations to be a little warmer than the reference simulations.

The RMSE varied greatly between simulations during the day (Fig. 4). The test runs have smaller RMSE values than the reference runs except at the southern lane for the sensor 1 that was probably the most exposed to the sun. For the northern lane, the forecasts using sensors 1 and 3 have the

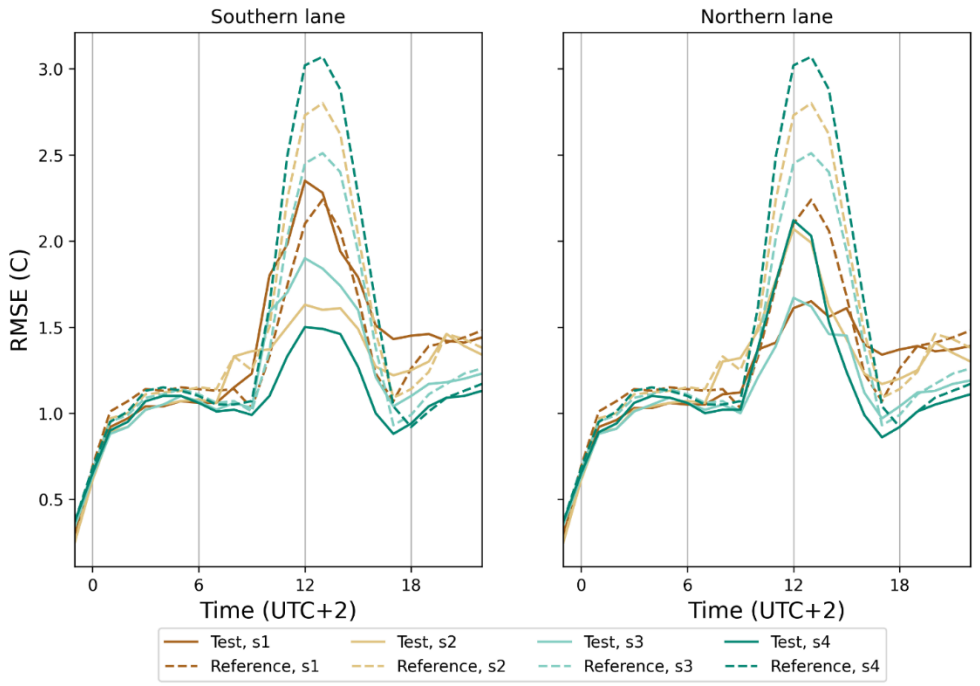

Fig. 4. Same as Figure 3 but for RMSE.

smallest RMSE values, whereas on the southern lane the forecasts for sensors 2 and 4 give the best values. However, it is still difficult to know which sensor is located on which lane as the forecast error is affected by many factors. During the night at the start of the forecast the test runs have slightly lower RMSE values. However, at the evening 17:00 local time the test simulations for sensors 1-3 have higher RMSE values than the reference simulations. At this time in the evening the bias in the reference simulation has already turned negative so the model cools too fast, but the observed temperature still matches better to the reference run than to the even colder test run.

In general, the verification results were quite dependent on the location, month and the time of the day. In October and March during the day the screening often made the already too cold forecast even colder. However, at best the shadowing algorithm decreased considerably the warm bias during the day. Only a short overview of the research results was given here, but there will be a more excessive publication about the results in the future. The data and results are available in the FMI data repository METIS [11]

Acknowledgements

The support provided by the following projects is gratefully acknowledged: Winter Premium funded by the European Regional Development Fund, the Arctic Airborne 3D project by Interreg Nord, and the 5G-Safe-Plus project, which is part of Eureka cluster Celtic Next initiative, funded in Finland by Business Finland.

References

[1] Steyn D.G.,**1980**. The calculation of view factors from fisheye-lens photographs: Research note, *Atmos.-Ocean*, 18(3), 254-258, *https://doi.org/10.1080/07055900.1980.9649091*.

[2] Jiao, Z.H. et al., **2019**. Evaluation of four sky view factor algorithms using digital surface and elevation model data. *Earth and Space Sci.*, **6(2)**, 222-237, *https://doi.org/10.1029/2018EA000475*.

[3] Chapman, L., et al. **2001b**. Modelling of road surface temperature from a geographical parameter database. Part 2: Numerical. *Meteorol. Appl*, 8(4), 421-436, *https://doi.org/10.1017/S1350482701004042*.

[4] Kršmanc, R., et al. **2014**. Upgraded METRo model within the METRoSTAT project. In Proc. of the 17th SIRWEC Conference, 8 pp.

[5] National Land Survey of Finland, **2021a**. Laser scanning data 2008 – 2019**.** Accessed 24 March 2022, *http://www.nic.funet.fi/index/geodata/mml/laserkeilaus/2008_latest/Laser_scanning_data_2008-2019_NLS.pdf*.

[6] Isenburg M., **2020**. LAStools - efficient LiDAR processing software, Accessed 24 March 2022, *http://rapidlasso.com/LAStools*.

[7] Huld T., et al., **2007**. r.horizon, GRASS GIS 8.0.1dev Reference Manual. Accessed 18 February 2022, *https://grass.osgeo.org/grass80/manuals/r.horizon.html*.

[8] Kangas M, et al., **2015**. RoadSurf – a modelling system for predicting road weather and road surface conditions. *Meteorol. Appl*. 22, 544–533, *https://doi.org/10.1002/met.1486*

[9] Senkova, A., et al. **2007**. Parametrization of orographic effects on surface radiation in HIRLAM. *Tellus A: Dyn. Meteorol. Oceanogr*, 59(3), 279-291, *https://doi.org/10.1111/j.1600-0870.2007.00235.x*.

[10] Frogner I.L., et al., **2019**. HarmonEPS—The HARMONIE Ensemble Prediction System. *Wea. Forecasting*, 34(6), 1909-1937, *https://doi.org/10.1175/WAF-D-19-0030.1* .

[11] Karsisto V., M. Horttanainen, **2022**. Study about effects of sky view factor and screening on road surface temperaure forecast accuracy [Data set], Finnish Meteorological Institute, accessed 25 March 2022, *https://doi.org/10.23728/FMI-B2SHARE.EBEE87254DAF41E6B2D3BCD6C32250C2* .